JACS
JOURNAL OF THE AMERICAN CHEMICAL SOCIETY
Article
pubs.acs.org/JACS

Proton-Coupled Electron Transfer Constitutes the Photoactivation Mechanism of the Plant Photoreceptor UVR8

Tilo Mathes,*,† Monika Heilmann,‡ Anjali Pandit,†,§ Jingyi Zhu,† Janneke Ravensbergen,† Miroslav Kloz,† Yinan Fu,‡ Brian O. Smith,‡ John M. Christie,‡ Gareth I. Jenkins,*,‡ and John T. M. Kennis*,†

†Biophysics Section, Department of Physics and Astronomy, Faculty of Sciences, VU University, De Boelelaan 1081, 1081 HV Amsterdam, The Netherlands

‡Institute of Molecular, Cell and Systems Biology, College of Medical, Veterinary and Life Sciences, Bower Building, University of Glasgow, Glasgow G12 8QQ, United Kingdom

§Department of Solid-State NMR, Leiden Institute of Chemistry, Leiden University, Einsteinweg 55, 2333 CC Leiden, The Netherlands

Supporting Information

ABSTRACT: UVR8 is a novel UV-B photoreceptor that regulates a range of plant responses and is already used as a versatile optogenetic tool. Instead of an exogenous chromophore, UVR8 uniquely employs tryptophan side chains to accomplish UV-B photoreception. UV-B absorption by homodimeric UVR8 induces monomerization and hence signaling, but the underlying photodynamic mechanisms are not known. Here, by using a combination of time-resolved fluorescence and absorption spectroscopy from femto- to microseconds, we provide the first experimental evidence for the UVR8 molecular signaling mechanism. The results indicate that tryptophan residues at the dimer interface engage in photoinduced proton coupled electron transfer reactions that induce monomerization.

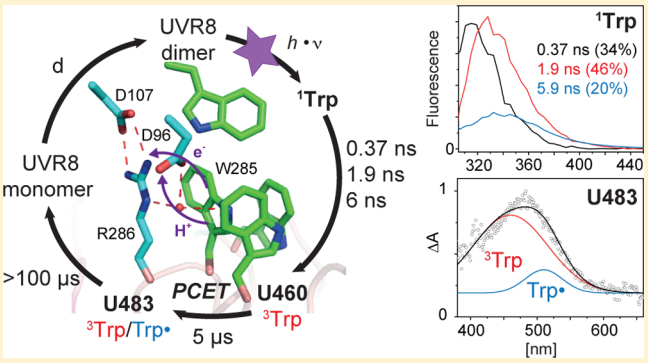

INTRODUCTION

The UV-B photoreceptor protein UVR8 (UV RESISTANCE LOCUS 8) from *Arabidopsis thaliana* employs the UV absorbing nature of tryptophan side-chains (Trp) to perceive UV-B (280−315 nm) radiation.[1−3] UVR8 is a dimeric protein in the dark-adapted state and undergoes UV-B induced monomerization both in vivo and in vitro with a quantum yield of about 20%.[1,2,4] Photoreception leads to rapid nuclear accumulation of UVR8,[5] where it orchestrates the expression of probably over 100 genes.[6,7] UV-B also promotes interaction between UVR8 and COP1 (CONSTITUTIVELY PHOTOMORPHOGENIC 1)[7] via the C-terminal, so far structurally undetermined C27 region of UVR8.[8] Because no secondary structural changes of this region are associated with monomerization, C27 likely becomes more exposed for interaction in the monomer.[4] Crystal structures show that the protein consists of a homodimer of 7-bladed β-propeller monomers (Figure 1A,B).[1,3,9] The dimer is maintained by a network of cross-dimer salt-bridges of which the ones between D96/D107 and R286 are particularly important for dimerization (Figure 1C).[1,3,4,10] Among the many aromatic amino acids at the dimer interface three Trp residues (W233, W285, W337) form the base of a pyramid with the tip provided by W94 in the adjacent monomer (Figure 1C). These Trps are excitonically coupled[1] and W233 and W285 are essential for UV-B mediated signaling in vivo.[1,11,12] In addition, three Trps and two tyrosine residues (W198, W250, W302, of the same monomer, Y201 and Y253) are located within 3.5−9 Å (Figure 1A,B,C). On the 7-bladed β-propeller, six additional Trp residues are located more remotely from the Trp pyramid within ∼15 Å (Figure 1A,B) and a final Trp is found on the C-terminal extension C27.

Recently, a time-resolved fluorescence spectroscopic study showed that in the dimer the excited state lifetime of the Trps becomes unquenched upon monomerization or by disruption of the excitonically coupled Trp pyramid by the W285F mutation.[13] The monomer is characterized by increased[3] and red-shifted Trp fluorescence[4] (Figure 1D). Although the light-induced increase in fluorescence is also observed in the constitutive monomeric mutant UVR8^{R286A}, the red shift apparently is a consequence of the light-induced rearrangement of the cross-dimer salt bridge network.[4]

One proposed mechanism of light-induced monomerization is electron transfer (ET) from the excited pyramid to the adjacent salt-bridge arginines. The resulting charge neutraliza-

Received: February 3, 2015
Published: May 8, 2015

ACS Publications © 2015 American Chemical Society

DOI: 10.1021/jacs.5b01177
J. Am. Chem. Soc. 2015, 137, 8113−8120

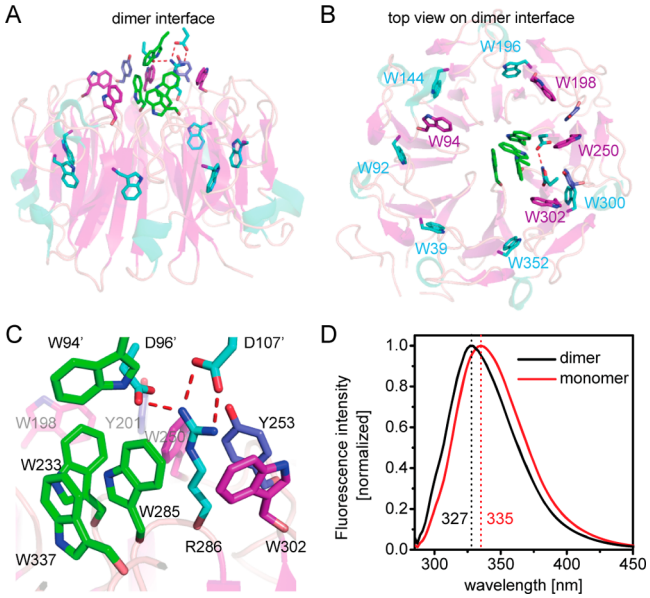

Figure 1. Molecular structure of UVR8 in its dimer form. The tertiary structure and details of one monomer and selected residues of the other monomer are displayed. (A) View across the dimer interface. (B) Top view on the dimer interface. (C) UVR8 forms excitonically coupled tryptophan pyramids (green) across the dimer interface via W94. Additionally, tryptophan residues are present close to the pyramid at the dimer interface (magenta) and further away in the seven bladed β-propeller structure (cyan). (C) Most likely, UV-B light is terminally perceived by the tryptophan pyramid and causes disruption of the adjacent arginine/aspartate cross-dimer salt-bridges. (D) Upon monomerization the tryptophan fluorescence shifts by about 8 nm to the red.

tion would lead to a disruption of the cross dimer salt bridges and thus dimer dissociation.[1,14,15] Alternatively, cation$-\pi$ interactions between the Trps and arginine may be perturbed upon electronic excitation.[3] In addition, the formation of a charge separated state by ET between W233 and W285 was recently proposed to induce breakage of the adjacent salt bridges by its strong dipole moment.[16] Monomerization takes place with a time constant of 200 ms after an initial conformational change with a time constant of 50 ms.[17]

Here, we studied the photodynamics of UVR8 by time-resolved absorption and fluorescence spectroscopy. With the application of these methods sensitive for the electronic and molecular nature of Trp, we give a first description of the primary photochemical events following UVR8 excitation in both dimer and monomer states.

RESULTS

Time-Resolved Fluorescence Spectroscopy. To investigate the excited-state dynamics of the UVR8 dimer, streak camera experiments were carried out with excitation of Trp at 280 nm, and detecting fluorescence in a spectral window between 300 and 500 nm. Figure 2A shows kinetic traces at selected wavelengths. At 310 nm, the signal has a major decay on a time scale of a few hundreds of ps. Upon going to longer wavelengths, the amplitude of this component decreases and the decay becomes progressively slower, until at 380 nm, little decay occurs on the 1.5 ns time window of the experiment. The kinetics show a significant amplitude before zero time through the back sweep of the streak camera,[18] which indicates that decay components longer than the time base of 1.5 ns contribute to the fluorescence dynamics.

Global analysis in terms of a model of parallel decaying components indicated four lifetimes of 14.7 ps, 370 ps, 1.9 ns, and 5.9 ns. The 14.7 ps component was rather unstructured and is likely to represent an excitation scattering contribution and is not considered further. Figure 2B shows the remaining decay associated spectra (DAS) with their contributions to the overall fluorescence decay. The 1.9 ns component dominates the fluorescence decay and has a maximum at 330 nm. The 5.9 ns component has smaller amplitude and is red-shifted with a maximum at 340 nm. The 370 ps component is clearly blue-shifted with respect to the 1.9 ns component, with a maximum at 315 nm. We note that the fitted lifetimes and DAS amplitudes are not very well determined, as single lifetimes can be fixed within rather broad boundaries without strongly affecting the quality of fit (Supporting Information Figure S1). Nevertheless, the overall picture emerges of a blue-shifted fast phase of 150−400 ps, a dominant middle phase of 1−2 ns and red-shifted slow phase of 5−6 ns. We conclude that three temporally and spectrally distinct phases can be identified in the excited-state dynamics of the UVR8 dimer. These clear

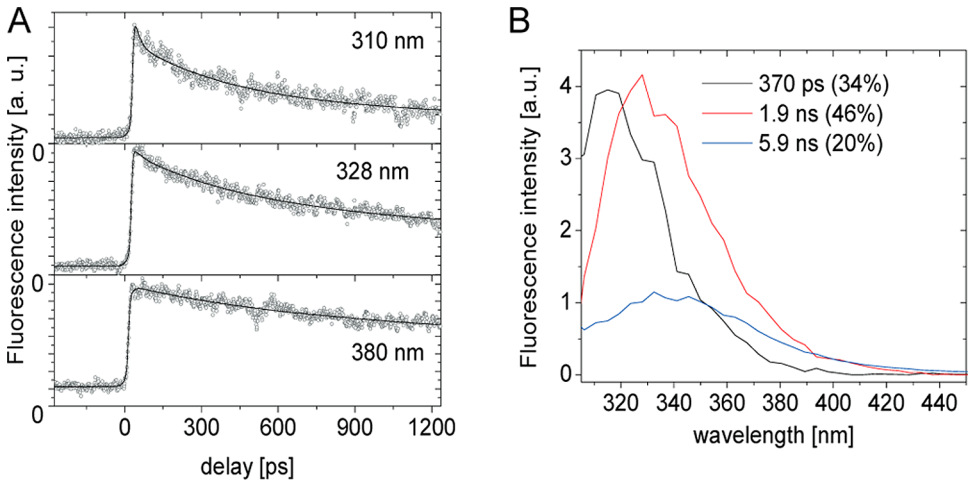

Figure 2. Time resolved fluorescence of the UVR8 dimer. (A) Fluorescence transients at selected wavelengths illustrating the decay of the corresponding DAS. (B) DAS and their corresponding lifetimes and fractions.

DOI: 10.1021/jacs.5b01177
J. Am. Chem. Soc. 2015, 137, 8113−8120

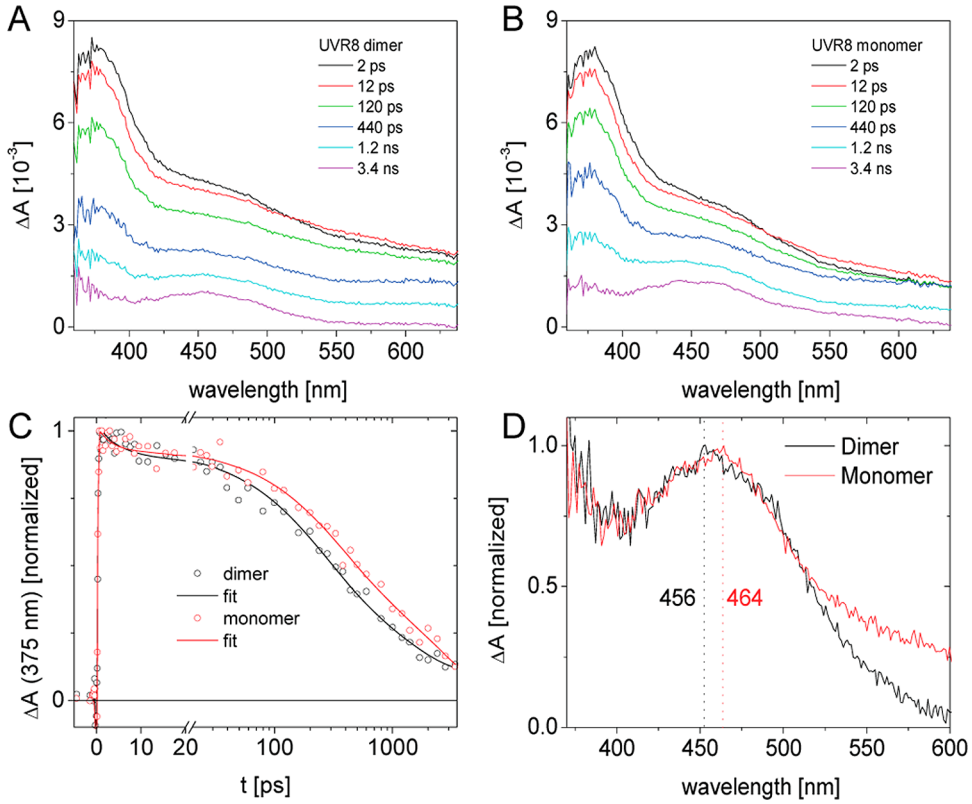

Figure 3. (A) Ultrafast photodynamics of UVR8 in its dimer state and (B) UVR8 monomer state after excitation at 266 nm illustrated by difference spectra at the indicated delays. Difference spectra at selected time delays after excitation of dimer and monomer, respectively. (C) Transient absorption change at 375 nm illustrates tryptophan excited state decay. (D) Transient absorption change at 460 nm illustrates the evolution into the nondecaying species.

subpopulations are not reflected in steady state fluorescence excitation spectra (Supporting Information Figure S2).

In the constitutively monomeric mutant UVR8^{R286A}, only two components were determined due to the limited signal-to-noise ratio (Supporting Information Figure S3). Also, a 487 ps component is observed that is clearly blue-shifted with respect to the 4.1 ns component suggesting that similar reaction processes take place in dimer and monomer following excitation.

Transient Absorption Spectroscopy: Femtosecond to Nanosecond Dynamics. In order to identify spectral signatures of reaction intermediates and putative signaling states, we performed time-resolved transient absorption spectroscopy. The application of high-energy photons to aqueous solutions leads to photoionization of water resulting in solvated electron species that show a broad unstructured absorbance and usually live for nanoseconds to microseconds.[19] Background correction was carried out by subtracting the transient absorption of buffer measured under the same conditions from the corresponding data sets (Supporting Information Figure S4A).

UVR8 Dimer and Monomer. Figure 3A illustrates the spectral evolution of the UVR8 dimer between 350 and 650 nm within the first 3.5 ns after excitation at 266 nm. Due to the slow recovery of the dimer in vitro (~48 h[1,3]), only data sets that still contained <10% of monomer were used (as judged by monitoring the dimer status by SDS PAGE or by emission spectra). Then, 2 ps after excitation, a typical Trp excited state spectrum is observed featuring a prominent absorbance at 375 nm, a broader contribution declining toward the red and a shoulder-like feature between 420 and 500 nm.[19,20] The overall absorbance within this spectral region gets broader within the first 20 ps and decays within the time scale of the experiment with a distinct absorption at 457 nm remaining. According to the fluorescence lifetime of UVR8 we expect that a fraction of excited-state absorption is still underlying the absorption.

Trp in solution forms a protonated Trp triplet on this time scale, that characteristically absorbs at ~420 nm and is clearly different from the species formed in UVR8 (Supporting Information Figure S4B).[19] According to its maximum absorption at ~460 nm the intermediate formed in UVR8 most likely resembles a neutral Trp triplet and is henceforth named U460.[21]

For the monomer, fully photoconverted samples were used. The UVR8 wild-type monomer shows a very similar spectral evolution, however, with altered kinetics (Figure 3B). The kinetic trace at 375 nm clearly shows that the excited state decays faster in the dimer, especially at delays >100 ps (Figure 3C). This observation is consistent with increased fluorescence of the monomer.[3,4,13]

Transient Absorption Spectroscopy: Nanosecond to Microsecond Dynamics. Several cross-dimer interactions have to be broken to create the signaling active monomer. Therefore, it is necessary that a signaling state perturbing these interactions is maintained sufficiently long to prevent their reformation. In other photoreceptor proteins signaling states may persist up to hours, but in terms of protein dynamics, even microsecond to millisecond lifetimes may suffice to induce global state transitions.[22] To address this time window, we performed transient absorption spectroscopy in the nano-

DOI: 10.1021/jacs.5b01177
J. Am. Chem. Soc. 2015, 137, 8113−8120

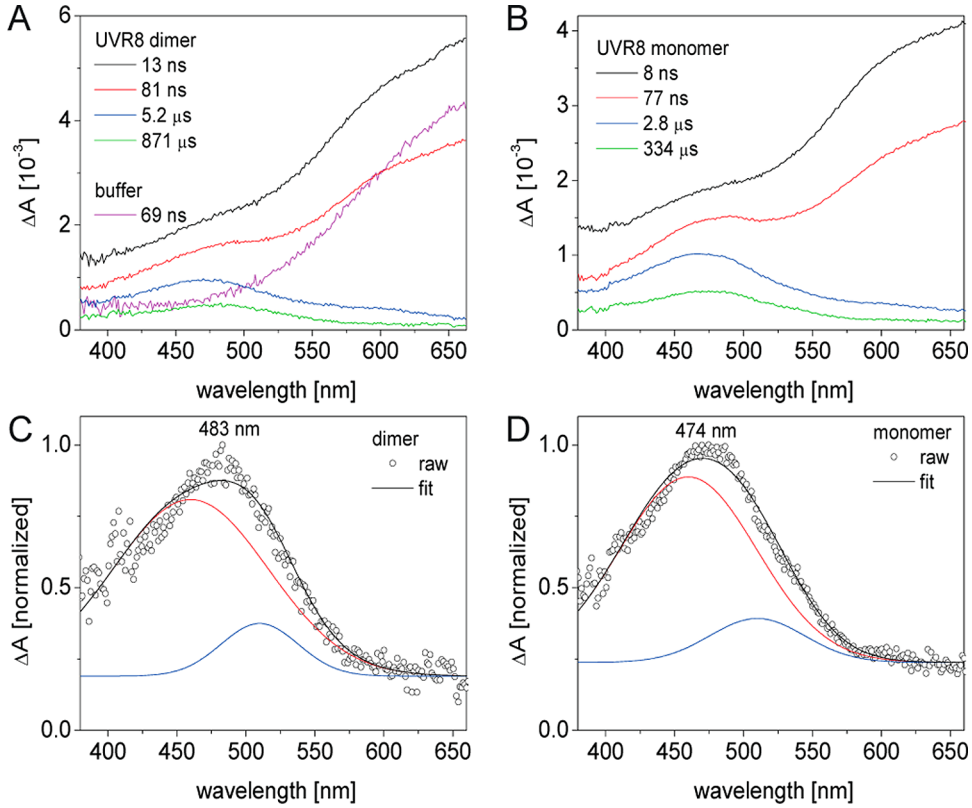

Figure 4. Photodynamics of UVR8 in the ns to μs time domain after excitation at 280 nm visualized by EADS for UVR8 (A) dimer and (B) monomer. (C,D) Difference spectra 120 μs after excitation and Gaussian fits using two functions peaking at 460 and 510 nm.

second to microsecond time domain using two electronically synchronized fs lasers.[23] We used an excitation wavelength of 280 nm and recorded the spectral evolution between 380 and 660 nm up to 125 μs (Figure 4). The contribution of the solvated electron artifact is significantly higher here, most likely due to resonant two-photon excitation of the Trp side chains at this wavelength (Supporting Information Figure S5). Because generation of Trp radicals under these conditions may also lead to a more complex artifact as recorded in buffer alone, no background correction was performed.

The spectral evolution of the UVR8 dimer was globally analyzed using a sequential reaction scheme with four components to adequately describe the data. The first evolution associated difference spectrum (EADS) (Figure 4A, black) has a lifetime of 13 ns and contains a strong underlying absorption of the buffer artifact starting from ~470 nm and with rising absorption toward the red edge of the observed spectral range. Additionally, a shoulder is visible at ~470 nm, which corresponds to the absorption of the U460 intermediate (see above). The spectrum loses amplitude and evolves into the spectrally similar red EADS, which lives for 81 ns. It still contains a significant contribution of the solvated electron artifact, which has a lifetime of 69 ns as observed in buffer alone (Figure 4A, magenta, Supporting Information Figure S5). Due to the loss of solvated electron contribution, the former shoulder at 470 nm becomes more prominent in the red EADS (see also in the normalized EADS, Supporting Information Figure S5), which subsequently evolves into a distinct peak at 470 nm in the next EADS (Figure 5A, blue). The spectrum is red-shifted compared to the final species observed on the ultrafast time scale and indicates further spectral evolution. It additionally contains a broad absorption on the red side of the 470 nm peak that declines toward longer wavelengths and is spectrally and kinetically different from the solvated electron contribution. In the decay associated difference spectra (DADS) (Supporting Information Figure S5), this absorption is attributed to the 5.2 μs decay in parallel with the U460 species, henceforth named U600.[21,24] Because the magnitude of the artifact species is significantly higher after excitation at 280 nm than at 266 nm (Supporting Information Figure S6) and because such a spectral feature is not observed in the ultrafast data set, we consider it an artifact formed by photoinduced electron ejection by resonant two-photon absorption of Trp side chains and generation of Trp radical cations under these conditions, which decays in 5.2 μs to the reduced state.[21,25] The final EADS (Figure 4A, green) is formed in 5.2 μs and is characterized by a peak at 483 nm and an almost complete loss of the broad absorption in the red. It lives for hundreds of microseconds and is henceforth named U483.

The spectral evolution of the UVR8 monomer is described using an identical global model (Figure 4B). The evolution on the <100 ns time scale is spectrally and kinetically similar to the dimer due to the dominant contribution of the solvated electron artifact in this time domain. The blue EADS with a lifetime of 2.8 μs is slightly blue-shifted (468 nm) in the monomer and also features the U600 absorption. In the final EADS attributed to U483 the peak shifts only to 474 nm. For Trp in aqueous solution, an intermediary species absorbing at ~470 nm is formed that red-shifts to 520 nm (Supporting Information Figure S5C) and represents the formation of a neutral Trp radical from the triplet state. The dynamics of U483 and U600 are also illustrated by the transient absorption change at selected wavelengths in Supporting Information Figure S7.

DOI: 10.1021/jacs.5b01177
J. Am. Chem. Soc. 2015, 137, 8113−8120

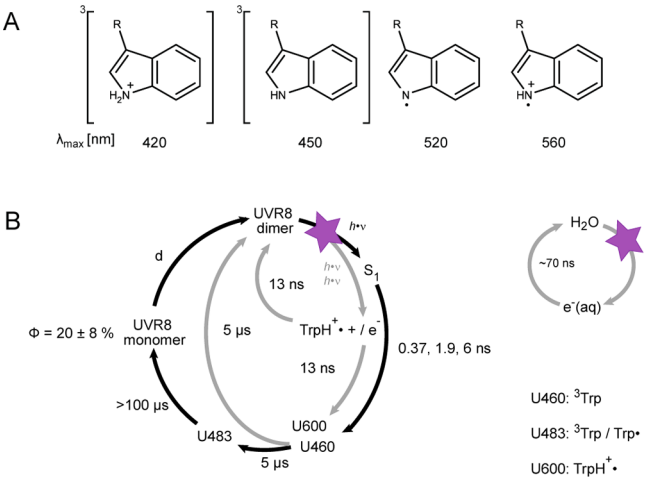

Figure 5. (A) Tryptophan triplet and radical species and their maximum absorption: cationic triplet;[19] neutral triplet;[24] cationic radical;[21] neutral radical.[30] (B) Tentative photocycle of UVR8 photoactivation as observed in vitro. After UV-B excitation solvent relaxation/solvation takes place in the excited state within few ps. Subsequently U460 and U600 are formed on the few-hundred-picosecond to few-nanosecond time scale. Within 5 μs, U483 is formed and lives for several 100 μs. The resulting UVR8 monomer redimerizes within a couple of days. Additionally, solvated electrons are generated from the aqueous medium and the sample.

■ DISCUSSION

In this study we investigated the photodynamics of UVR8 in its dimeric form and its monomeric state by means of time-resolved fluorescence and absorption spectroscopy from the femtosecond time scale to that of 100 μs. Applying transient spectroscopy using excitation wavelengths in the UV range is especially challenging due to the generation of solvated electron species from the aqueous medium. Additionally, the extremely long recovery from the activated, monomeric state to the dark-adapted dimeric state (~48 h) limits the signal-to-noise ratio. Nevertheless, we derive clear dynamic and spectral information on the primary photochemical events associated with UVR8 activation. All experiments were conducted under aerobic conditions, similar to the native environment in the plant cell.

Excited State Dynamics of UVR8. The streak camera data on the WT dimer clearly indicated three distinct phases in fluorescence decay: a DAS at 315 nm with a lifetime of 370 ps, a DAS at 326 nm with a lifetime of 1.9 ns, and a DAS at 340 nm with a lifetime of 5.9 ns, with relative contributions of 34%, 46%, and 20%, respectively. These data compare well with the ultrafast transient absorption data, which indicated a fast phase in the excited-state decay in the hundreds of picoseconds that accounted for about half the population, whereas the remainder of the excited states decay on the nanosecond time scale. Within the experimental error and given the different excitation conditions (280 nm for the streak camera, 266 nm for the transient absorption), these results are mutually consistent.

Liu et al.[13] assigned a 150 ps fluorescence decay component detected at 360 nm in the UVR8 dimer to a reactive phase that constitutes the primary event for UVR8 monomerization, originating from a reaction at the excitonically coupled Trp pyramid. The 370 ps component that results from the streak camera experiments corresponds to such a phase given the boundaries of the fit as outlined above: here, we identify its complete spectral signature and conclude that it is blue-shifted to 315 nm as compared to the other emitting Trps in UVR8. The 370 ps component contributes 34% of the overall fluorescence decay. Assuming nonselective excitation at 280 nm, it would correspond to the fluorescence of 4.7 Trps, which agrees quite well with the number of Trps that constitute the pyramid. Also, the amplitude of its DAS at 360 nm (23% of the total decay) is identical to that of Liu and co-workers.[13]

Interestingly, we observe similar fluorescence spectra and timing for the constitutive monomer $UVR8^{R286A}$, which suggests that the few hundred picoseconds component is not an exclusive property of the dimer. In this regard, it is important to note that in Trp fluorescence, such decay time constants are frequently observed in proteins resulting of rotameric states of the indole side chain that favor quenching of the Trp excited state by the backbone amides through ET.[26−28] Therefore, it cannot be excluded that the 370 ps component in UVR8 dimer results from such phenomena.

In transient absorption we observe a slower excited state decay in monomer than in the dimer, in line with the observation of Liu et al. The spectra of the long-lived U483 intermediates are almost identical in dimer and monomer with minor shifts of their maximum absorption, indicating that similar photoproducts are formed. A clear analysis of the differences between dimer and monomer forms is not trivial due to the lack of selectivity of the excitation, as all 14 Trp residues in each monomer have strongly overlapping absorption spectra. Half of the Trp residues are situated at the dimer interface and their environment may change upon monomerization, which means that only 50% of the excited indole side chains that we observe potentially account for the differences between dimer and monomer. In addition, the photoinduced reactions may not be exclusive to the dimer state and are likely to occur in the monomer as well.

Intermediates in UVR8 Photoactivation. The transient absorption of UVR8 reflects the photoinduced chemical changes in the protein. Current ideas on the light-activation of UVR8 include photoinduced ET within the Trp pyramid or to nearby arginines, or simply changes in the cation−π interaction between the excited Trps of the pyramid and adjacent arginines to disrupt the cross-dimer salt-bridges.[1,3,14−16] Such reactions may be facilitated by singlet and triplet excited states and result in the formation of Trp radical species that exhibit characteristic spectroscopic properties in the monitored spectral range (Figure 5A). Arginine radicals typically absorb at 320 nm and are not resolved here.[29] Using transient absorption spectroscopy, we observed the spectral intermediates U460 and U483. Additionally, a U600 species is observed between 500 and 650 nm that decays in 3−5 μs and is considered an artifact of two-photon resonant ionization. Considering the spectral and kinetic properties of these intermediates, we discuss the molecular identities of U460 and U483.

U460 may be attributed to a Trp triplet state. Indole triplet states in neutral or cationic forms are formed within 10 ns time scale from the singlet excited state. The neutral form absorbs strongly (ε_T = 5000 M^{-1} cm^{-1}) at ~450 nm[24,31] whereas the cationic triplet absorbs at ~420 nm.[19,24] The latter is likely formed via singlet excited state proton uptake and simultaneous intersystem crossing (ISC) and is observed for Trp in solution (Supporting Information Figure S4,[19,32]) but not for UVR8. Under anaerobic conditions the neutral triplet lifetime of Trp in solution varies between 12 and 40 μs,[24] but lifetimes in the 100 μs range have also been reported.[33] The absorption maximum

DOI: 10.1021/jacs.5b01177
J. Am. Chem. Soc. 2015, 137, 8113−8120

of 460 nm and lifetime of 2−5 μs therefore indicate a Trp neutral triplet state for U460.

The assignment of U483 is less straightforward. Its absorption maximum appears too red-shifted for a Trp triplet state. On the other hand, its absorption appears too blue-shifted for assignment to a Trp cationic or neutral radical: the Trp neutral radical absorption maximum may lie between 510 and 550 nm,[21] depending on its molecular environment.[30] Trp cationic radicals absorb near 560 nm. Both forms have significantly weaker absorption than the neutral triplet state (ε_R = 1800 M^{-1} cm^{-1}).[34] Trp radicals are formed from Trp singlet or triplet excited states by photoinduced ET resulting in a cationic radical and subsequent proton transfer (PT) for a neutral radical. Trp in solution forms neutral radicals absorbing at ∼516 nm under these conditions (Supporting Information Figure S7).

Considering the above, it is quite obvious that U483 does not correspond to a single molecular species. Given the large number of Trps in UVR8, it is likely that U483 represents a mixture of particular Trp reaction products that may or may not be coupled to the monomerization reaction. Indeed, spectral fitting of both the dimer and monomer U483 spectra shows that the spectral features can be approximated by a mixture of a Trp triplet state absorbing at 460 nm and a Trp neutral radical at 510 nm (Figure 4C,D), with the amplitude of the triplet about three times higher than that of the neutral radical. Given that the extinction coefficient of the Trp triplet state is about 3 times higher than that of the neutral radical, the contributions of triplet and neutral radical in terms of transient concentration are about equal. On the time scale of our experiment U483 is considered nondecaying. It is conceivable that triplet state and radical decay with different rates that, however, cannot be resolved in the present data.

The presence of oxygen in our experiments may lead to reactive oxygen species (ROS) generation from the Trp triplet states that in principle could be relevant for signal generation. The long lifetimes for the observed triplet species, however, do not suggest any significant photosensitizing effect. Moreover, it was previously shown that the presence of ROS or reductive agents does not influence the monomerisation reaction.[3]

UVR8 Reaction Mechanism. The photodynamics of the Trp ensemble in UVR8 can be summarized as illustrated in Figure 5B. We observe excited state decay in the few-hundred-picoseconds to nanoseconds time domain to the triplet intermediate U460. In parallel, solvated electron generation from the aqueous buffer and Trp takes place after resonant two-photon absorption, which accounts for the formation of Trp radical cations (U600) with a lifetime of 5 μs. The solvated electrons disappear with lifetimes of 13 and 81 ns. U460 decays and evolves in 5 μs into U483, which exhibits overall lower amplitude with respect to U460 and is assigned to a mixture of Trp triplet and neutral radical states. U483 lives for >100 μs and is a candidate for the signaling state.

A key question is which Trps give rise to the observed spectroscopic signals and how the species identified relate to the photoreception mechanism of UVR8. Present knowledge of UVR8 structure and of amino acids involved in photoreception,[11] together with computational modeling of the photoreception mechanism,[14−16] indicate that Trps in the dimer interface, rather than the ones on the β-propeller blades, will be responsible for spectroscopic signals associated with photoreception. Moreover, according to our spectroscopic assignment we expect ET and PT from the Trps to take place, consistent with recently proposed models.[14,15]

The pyramid base formed by W233, W285, and W337 is flanked by the cross-dimer salt-bridges between R286/D96/D107 and R338/E43/D44 (Supporting Information Figure S8A,B). Both arginine residues are within ∼5 Å of W285 and their electronic π systems are oriented parallel (R286) and almost coplanar (R338) to it and thereby allow for efficient orbital overlap for ET. Additionally, W233 is close to R234 that is involved in an intramonomer salt-bridge to E182. The π electronic systems of W233 and R234 are arranged almost perpendicular. None of the base Trps are in direct contact with the carboxylic residues of the cross dimer salt-bridges, except for W285, connected to D96 via a single water molecule that also bridges D96 and R286. W94 that forms the pyramid tip is, however, directly H-bonded to D96 and in close proximity to R99, which is not involved in the cross-dimer salt-bridge network (Supporting Information Figure S8C). The nearby R286 is oriented in perpendicular fashion regarding the π electronic system of W94. Functional studies on site-directed mutants have revealed the essential roles of W285 and W233 in UVR8 photoreception[11,17] and computational models highlight the likely importance of ET and PT in the reaction mechanism.[14−16] Therefore, it is credible to propose that the Trp species identified from our spectroscopic observations correspond with events that are fundamental to the photoreception mechanism. A possible model is that formation of U483 from the triplet state U460 represents photoinduced ET from W285 to R286 in concert with PT to D96 via a bridged water molecule, resulting in a W285 neutral radical, and the neutralized salt bridge (Figure 6). This model is consistent with

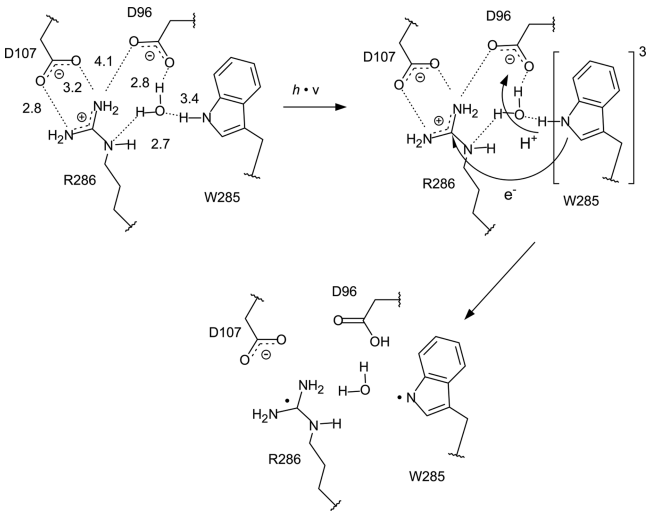

Figure 6. Photoinduced neutralization of the R286/D96 salt-bridge by ET and PT from W285.

recent quantum chemical calculations.[14,15] The similar pK_a values (∼4) of the intermediary Trp cation radical[24] and the carboxylic side chain provides a more likely scenario than induced PT from arginine (pK_a ∼12) to aspartate as alternatively proposed.[16] The resulting neutral radical is stable for hundreds of microseconds and prevents reversion of ET/PT and thereby reformation of the salt bridge and thus potential redimerization of UVR8. It is conceivable that rearrangements within the Trp pyramid subsequently take place and lead to ejection of the water molecule as recently observed by dynamic

DOI: 10.1021/jacs.5b01177
J. Am. Chem. Soc. 2015, 137, 8113−8120

crystallography.[12] We consider the triplet state contribution, which constitutes about half the population of U483 (Figure 5E) as a nonreactive fraction of long-lived triplets, probably residing on the buried Trps of the propeller blades (Figure 1).

However, two observations complicate the above interpretation. First, the photodynamics of the constitutively monomeric UVR8^{R286A} mutant and wild-type monomer are very similar to those of wild-type dimer. Therefore, the observed spectral intermediates do not require the presence of an intact Trp pyramid, which is disrupted in the monomer. Moreover, if the observed spectroscopic signals are associated with the mechanism of photoreception, then photoreception can occur in the monomer and is not uniquely associated with the dimer. Research to date has focused on the role of the UVR8 dimer in photoreception, but the possibility of monomer photoreception should not be excluded. Indeed, the initial structural changes observed by transient grating spectroscopy and fluorescence spectroscopy are also observed in constitutively monomeric mutants.[4,17] Second, in experiments with the UVR8^{W233F,W285F,W337F} mutant, which is deficient in UV-B responsiveness,[1] we observed similar ultrafast absorption spectra to wild-type over the microsecond time scale (Supporting Information Figure S9). This finding suggests that nonpyramid Trps can generate similar spectral intermediates. This is perhaps not surprising because the peripheral Trps in the dimer interface, W198, W250, and W302 (Figure 1, magenta) have similar molecular environments to those in the pyramid (Supporting Information Figure S8D−F), in that they are situated similarly in close proximity to essential and nonessential salt bridge residues, as discussed in recent computational studies.[14,15] As a consequence, we have to assume that, in wild-type UVR8, nonpyramid Trps also partially give rise to the observed spectroscopic signals. Hence, in future studies, it may be difficult to relate spectroscopic observations to the mechanism of photoreception even with extensive mutational analysis, and additional, high-resolution methods may be needed to determine the exact reaction mechanism.

No Indication for a Trp Light-Harvesting Antenna Function in UVR8. Considering the fact that only a few of the Trps (particularly W285 and W233) are crucial for the photoactivation in vivo[11] the role of the remaining Trps remains unclear. Liu and co-workers interpret the ns lifetimes observed in fluorescence as resonant energy transfer from the peripheral Trps to the Trp pyramid to accomplish light harvesting.[13] To address this issue, we measured fluorescence anisotropy of UVR8 to investigate whether randomization of the Trp emission dipoles occurs through energy transfer during the excited-state lifetime. The fluorescence anisotropy of UVR8 was determined by polarization dependent recording of the emission induced by exclusive excitation of the ^1L_a absorption band at 300 nm. The maximum anisotropy for immobilized Trp is 0.3,[35] whereas in proteins, slightly lower maximal anisotropies of 0.26 are usually observed,[36] caused by rotational diffusion of Trp rotameric states.[27,28] We found anisotropy values of 0.24 and 0.21 for UVR8 dimer and monomer, respectively. The high fluorescence anisotropy of 0.24 in the UVR8 dimer suggests that extensive resonant energy transfer among the Trp side chains does not occur. In addition, the streak camera results indicate all-positive DAS and, thus, suggest a minimal (if any) spectral overlap between donor emission and acceptor absorption and, thus, speak against energy transfer processes among different spectral Trp forms. The Trps found buried in the 7-bladed β-propeller structure are considered structurally important, as in other WD40-repeat proteins,[9] and are therefore unlikely to have evolved specifically as light-harvesting pigments in UVR8.

■ CONCLUSIONS

The photodynamics of UVR8 indicate the formation of Trp species that are stable on the 100 μs time scale and may be assigned to a mixture of Trp triplet and neutral radical states. The experimentally observed species are indicative of a light-induced proton-coupled electron transfer (PCET) mechanism involving Trp, Arg, and Asp at the dimerization interface that results in neutralization of salt bridge residues to induce monomerization. Evidence for a light-harvesting mechanism by resonant energy transfer from distal Trps to the Trp pyramid at the dimer interface has not been found.

■ EXPERIMENTAL PROCEDURES

Sample Preparation. Heterologous expression, mutation, and purification of UVR8 has been described.[1] For transient absorption spectroscopy, the sample was circulated through a flow-cell cuvette of 2 mm path length by a peristaltic pump with a speed of ∼20 mL/min, at a total volume of ∼10 mL. The sample concentration was adjusted to an OD_{280nm} of ∼4−5/cm. For the streak camera experiments, the sample was circulated through a rectangular flow-cell cuvette by a peristaltic pump with a speed of ∼4 mL/s. The excitation beam was passed close to the cuvette window so as to avoid self-absorption of the fluorescence. The OD_{280nm} was adjusted to 0.2/cm, at a total reservoir volume of 100 mL. All experiments were carried out under aerobic conditions.

Fluorescence Spectroscopy. Steady state fluorescence measurements were carried out using a Jobin Ivon HORIBA Fluorolog Tau-3 lifetime system. UVR8 samples were diluted to a total volume of 2 mL to an OD_{280nm} ∼0.05/cm in a stirred 1 × 1 cm quartz cuvette. Fluorescence anisotropy measurements were carried out with emission and excitation slits set to 5 nm, respectively. Emission spectra using 300 nm excitation were recorded from 310 to 400 nm.

Transient Absorption Spectroscopy. Transient absorption spectroscopy was performed on a setup using two electronically synchronized amplified Ti:sapphire laser systems (Legend and Libra, Coherent, Mountain View, CA) as described.[23] The wavelength of the excitation beam was set to 266 or 280 nm by third harmonic generation of the fundamental wavelength of the Ti:sapphire laser or second harmonic generation of the 560 nm output of the OPA. Pump pulse energies were set to 600 nJ per pulse unless otherwise stated. A broadband probe beam was generated by focusing part of the output of the Libra on a CaF_2 plate. The TAS signal was acquired as described by Berera et al.[37] The time difference between pump and probe was controlled in two ways. A delay line was used for delays of the pump beam in the femtosecond to nanosecond regime. Delay steps of 12.5 ns were generated by selection and amplification of consecutive seed pulses of the oscillator.[23] Both delay methods were applied independently.

Streak Camera. Time-resolved tryptophan fluorescence was recorded by using a synchroscan streak camera (Hamamatsu) as described previously in refs 27 and 28. A Coherent Vitesse-Rega system operating at 50 kHz equipped with an OPA was employed for excitation. Excitation pulses at 280 nm were provided by frequency doubling of the 560 nm output of the OPA. The excitation power was lower than 0.1 mW. The time base was 1.5 ns long, and the time resolution approximately 7 ps. The back-sweep of the streak camera was used to estimate fluorescence decay time constants longer than the time base.[18] The relative contributions to the total fluorescence decay of the DAS were calculated by integrating their respective intensities, thereby taking into account the quadratic dependence of the bandpass on the wavelength.

Data Analysis. Time resolved data was globally analyzed using the glotaran software package.[38] Because the wavelength sensitivity of the spectrograph/streak camera detection system was not separately

DOI: 10.1021/jacs.5b01177
J. Am. Chem. Soc. 2015, 137, 8113−8120

determined, the DAS that followed from global analysis were corrected by first calculating the integrated fluorescence for each wavelength following from the DAS and, subsequently, scaling the DAS for each wavelength to reproduce the steady-state fluorescence spectrum.

■ ASSOCIATED CONTENT

Supporting Information

Alternative fits for time resolved fluorescence data, steady-state absorption and fluorescence excitation spectra, time resolved fluorescence of the constitutive monomeric UVR8 mutant, additional data on the photodynamics of UVR8, UVR8 mutants and Trp in solution, molecular environment of the interfacial tryptophan residues are provided in the Supporting Information. The Supporting Information is available free of charge on the ACS Publications website at DOI: 10.1021/jacs.5b01177.

■ AUTHOR INFORMATION

Corresponding Authors

*t.mathes@vu.nl
*j.t.m.kennis@vu.nl
*Gareth.Jenkins@glasgow.ac.uk.

Author Contributions

The manuscript was written through contributions of all authors. All authors have given approval to the final version of the manuscript.

Notes

The authors declare no competing financial interest.

■ ACKNOWLEDGMENTS

M.H. and G.I.J. were supported by the Laserlab Europe access grant LCVU001825. J.T.M.K., J.Z., and T.M. were supported by the Chemical Sciences Council of The Netherlands Organization for Scientific Research its abbreviation (CW-NWO) through an ECHO and a VICI grant (to J.T.M.K.). J.R. was supported through the BioSolar Cells program. A.P. was supported by Harvest Marie Curie Research Training Network (PITN-GA-2009-238017) and a CW-NWO VIDI grant. M.H. and Y.F. were supported by grants from The Leverhulme Trust and the U.K. Biotechnology and Biological Sciences Research Council, respectively (to G.I.J., J.M.C., and B.O.S.).

■ REFERENCES

(1) Christie, J. M.; Arvai, A. S.; Baxter, K. J.; Heilmann, M.; Pratt, A. J.; O'Hara, A.; Kelly, S. M.; Hothorn, M.; Smith, B. O.; Hitomi, K.; Jenkins, G. I.; Getzoff, E. D. *Science* **2012**, *335*, 1492.
(2) Rizzini, L.; Favory, J. J.; Cloix, C.; Faggionato, D.; O'Hara, A.; Kaiserli, E.; Baumeister, R.; Schafer, E.; Nagy, F.; Jenkins, G. I.; Ulm, R. *Science* **2011**, *332*, 103.
(3) Wu, D.; Hu, Q.; Yan, Z.; Chen, W.; Yan, C.; Huang, X.; Zhang, J.; Yang, P.; Deng, H.; Wang, J.; Deng, X.; Shi, Y. *Nature* **2012**, *484*, 214.
(4) Heilmann, M.; Christie, J. M.; Kennis, J. T. M.; Jenkins, G. I.; Mathes, T. *Photochem. Photobiol. Sci.* **2015**, *14*, 252.
(5) Kaiserli, E.; Jenkins, G. I. *Plant Cell* **2007**, *19*, 2662.
(6) Brown, B. A.; Cloix, C.; Jiang, G. H.; Kaiserli, E.; Herzyk, P.; Kliebenstein, D. J.; Jenkins, G. I. *Proc. Natl. Acad. Sci. U.S.A.* **2005**, *102*, 18225.
(7) Favory, J. J.; Stec, A.; Gruber, H.; Rizzini, L.; Oravecz, A.; Funk, M.; Albert, A.; Cloix, C.; Jenkins, G. I.; Oakeley, E. J.; Seidlitz, H. K.; Nagy, F.; Ulm, R. *EMBO J.* **2009**, *28*, 591.
(8) Cloix, C.; Kaiserli, E.; Heilmann, M.; Baxter, K. J.; Brown, B. A.; O'Hara, A.; Smith, B. O.; Christie, J. M.; Jenkins, G. I. *Proc. Natl. Acad. Sci. U.S.A.* **2012**, *109*, 16366.
(9) Wang, Y.; Jiang, F.; Zhuo, Z.; Wu, X. H.; Wu, Y. D. *PLoS One* **2013**, *8*, e65705.
(10) Wu, M.; Strid, A.; Eriksson, L. A. *J. Chem. Inf. Model.* **2013**, *53*, 1736.
(11) Jenkins, G. I. *Plant Cell* **2014**, *26*, 21.
(12) Zeng, X.; Ren, Z.; Wu, Q.; Fan, J.; Peng, P.-P.; Tang, K.; Zhang, R.; Zhao, K.-H.; Yang, X. *Nature Plants* **2015**, *1*, 14006.
(13) Liu, Z.; Li, X.; Zhong, F. W.; Li, J.; Wang, L.; Shi, Y.; Zhong, D. *J. Phys. Chem. Lett.* **2014**, *5*, 69.
(14) Wu, M.; Strid, A.; Eriksson, L. A. *J. Phys. Chem. B* **2014**, *118*, 951.
(15) Li, X.; Chung, L. W.; Morokuma, K.; Li, G. *J. Chem. Theory Comput* **2014**, *10*, 3319.
(16) Voityuk, A. A.; Marcus, R. A.; Michel-Beyerle, M. E. *Proc. Natl. Acad. Sci. U.S.A.* **2014**, *111*, 5219.
(17) Miyamori, T.; Nakasone, Y.; Hitomi, K.; Christie, J. M.; Getzoff, E. D.; Terazima, M. *Photochem. Photobiol. Sci.* **2015**, 995−1004.
(18) van Stokkum, I. H.; Gauden, M.; Crosson, S.; van Grondelle, R.; Moffat, K.; Kennis, J. T. M. *Photochem. Photobiol.* **2011**, *87*, 534.
(19) Leonard, J.; Sharma, D.; Szafarowicz, B.; Torgasin, K.; Haacke, S. *Phys. Chem. Chem. Phys.* **2010**, *12*, 15744.
(20) Sharma, D.; Léonard, J.; Haacke, S. *Chem. Phys. Lett.* **2010**, *489*, 99.
(21) Bent, D. V.; Hayon, E. *J. Am. Chem. Soc.* **1975**, *97*, 2612.
(22) Eitoku, T.; Nakasone, Y.; Zikihara, K.; Matsuoka, D.; Tokutomi, S.; Terazima, M. *J. Mol. Biol.* **2007**, *371*, 1290.
(23) Ravensbergen, J.; Abdi, F. F.; van Santen, J. H.; Frese, R. N.; Dam, B.; van de Krol, R.; Kennis, J. T. M. *J. Phys. Chem. C* **2014**, *118*, 27793.
(24) Tsentalovich, Y. P.; Snytnikova, O. A.; Sagdeev, R. Z. *J. Photochem. Photobiol. A* **2004**, *162*, 371.
(25) Solar, S.; Getoff, N.; Surdhar, P. S.; Armstrong, D. A.; Singh, A. *J. Phys. Chem.* **1991**, *95*, 3639.
(26) Callis, P. R.; Liu, T. *J. Phys. Chem. B* **2004**, *108*, 4248.
(27) Larsen, O. F. A.; van Stokkum, I. H. M.; Pandit, A.; van Grondelle, R.; van Amerongen, H. *J. Phys. Chem. B* **2003**, *107*, 3080.
(28) Pandit, A.; Larsen, O. F. A.; van Stokkum, I. H. M.; van Grondelle, R.; Kraayenhof, R.; van Amerongen, H. *J. Phys. Chem. B* **2003**, *107*, 3086.
(29) Ito, T.; Morimoto, S.; Fujita, S.; Nishimoto, S. *Radiat. Phys. Chem.* **2009**, *78*, 256.
(30) Bernini, C.; Andruniow, T.; Olivucci, M.; Pogni, R.; Basosi, R.; Sinicropi, A. *J. Am. Chem. Soc.* **2013**, *135*, 4822.
(31) Volkert, W. A.; Kuntz, R. R.; Ghiron, C. A.; Evans, R. F.; Santus, R.; Bazin, M. *Photochem. Photobiol.* **1977**, *26*, 3.
(32) Sherin, P. S.; Snytnikova, O. A.; Tsentalovich, Y. P. *Chem. Phys. Lett.* **2004**, *391*, 44.
(33) Kowalska-Baron, A.; Chan, M.; Galecki, K.; Wysocki, S. *Spectrochim Acta, Part A* **2012**, *98*, 282.
(34) Bryant, F. D.; Santus, R.; Grossweiner, L. I. *J. Phys. Chem.* **1975**, *79*, 2711.
(35) Lakowicz, J. *Principles of Fluorescence Spectroscopy*; Kluwer Academic/Plenum Publishers: New York/Boston/Dordrecht/London/Moscow, 1999.
(36) Lakowicz, J. R.; Maliwal, B. P.; Cherek, H.; Balter, A. *Biochemistry* **1983**, *22*, 1741.
(37) Berera, R.; van Grondelle, R.; Kennis, J. T. M. *Photosynth. Res.* **2009**, *101*, 105.
(38) Snellenburg, J. J.; Laptenok, S. P.; Seger, R.; Mullen, K. M.; van Stokkum, I. H. M. *J. Stat. Software* **2012**, *49*, 1.

DOI: 10.1021/jacs.5b01177
J. Am. Chem. Soc. 2015, 137, 8113−8120